npj | microgravity

www.nature.com/npjmgrav

ARTICLE OPEN

Check for updates

Explainable machine learning identifies multi-omics signatures of muscle response to spaceflight in mice

Kevin Li[1,2,10], Riya Desai[3,10], Ryan T. Scott[1,4], Joel Ricky Steele[4,5,6], Meera Machado[7], Samuel Demharter[7], Adrienne Hoarfrost[8], Jessica L. Braun[9], Val A. Fajardo[9], Lauren M. Sanders[4,6]✉ and Sylvain V. Costes[4]✉

The adverse effects of microgravity exposure on mammalian physiology during spaceflight necessitate a deep understanding of the underlying mechanisms to develop effective countermeasures. One such concern is muscle atrophy, which is partly attributed to the dysregulation of calcium levels due to abnormalities in SERCA pump functioning. To identify potential biomarkers for this condition, multi-omics data and physiological data available on the NASA Open Science Data Repository (osdr.nasa.gov) were used, and machine learning methods were employed. Specifically, we used multi-omics (transcriptomic, proteomic, and DNA methylation) data and calcium reuptake data collected from C57BL/6 J mouse soleus and tibialis anterior tissues during several 30+ day-long missions on the international space station. The QLattice symbolic regression algorithm was introduced to generate highly explainable models that predict either experimental conditions or calcium reuptake levels based on multi-omics features. The list of candidate models established by QLattice was used to identify key features contributing to the predictive capability of these models, with Acyp1 and Rps7 proteins found to be the most predictive biomarkers related to the resilience of the tibialis anterior muscle in space. These findings could serve as targets for future interventions aiming to reduce the extent of muscle atrophy during space travel.

npj Microgravity (2023)9:90 ; https://doi.org/10.1038/s41526-023-00337-5

INTRODUCTION

Muscle atrophy, caused by prolonged exposure to microgravity conditions, is a major challenge faced by astronauts during spaceflight[1,2]. Although intense physical exercise is currently the main countermeasure, it requires a significant amount of time from each astronaut (2.5 hours per day, including equipment setup and breakdown), and even with exercise, the continuous exposure to microgravity cannot be fully offset.

It has been proposed that muscle atrophy may be at least partly explained by the dysregulation of cytoplasmic Ca^{2+} levels due to abnormalities in the Sarco Endoplasmic Reticulum Calcium ATPase (SERCA) pump's ability to reuptake cytoplasmic Ca^{2+} during muscle relaxation[1]. Mammalian muscles are broadly classified into two types: slow-twitch muscles composed predominantly of oxidative muscle fibers (e.g., postural muscles like the soleus [SOL], which is found in the calf and is important for resisting the pull of gravity) and fast-twitch muscles composed predominantly of glycolytic muscle fibers (e.g., explosive muscles like the tibialis anterior [TA], located in the shin). The SOL and TA are two of the primary muscles impacted by spaceflight, and previous studies have shown that both the murine SOL and TA will atrophy in response to microgravity exposure[1,3].

With respect to Ca^{2+} handling, recent work has shown that during spaceflight, Ca^{2+} uptake is impaired in the SOL muscle while being enhanced in the TA muscle, indicating that SERCA function is affected differently in the two muscle types[1]. However, the molecular mechanisms driving these aberrations in Ca^{2+} reuptake by SERCA are not very well elucidated. Additionally, as Ca^{2+} handling at the level of SERCA was not impaired in the TA, it is possible that there may be other molecular drivers of the muscle atrophy phenotype. Understanding these mechanisms at the molecular level is important for prevention and mitigation.

Machine learning (ML) methods are particularly effective in identifying patterns in complex biological data, particularly for discovering biomarkers in heterogeneous, high-dimensional, multi-omics datasets[4]. Compared to traditional statistical methods, ML methods are also less prone to distribution-specific effects[5], making them a promising alternative to classic systems biology. This is particularly important for space biological research, where small datasets are often combined to increase statistical power.

In this study, we present an ML-based approach to create a mapping between changes in multi-omics data (transcriptomic, proteomic, and epigenomic) and calcium reuptake in the SOL and TA muscles of mice that have been flown in space, compared to ground controls. To our knowledge, this approach has not been applied to this scientific question before.

When choosing an ML method for the purposes of gaining insight into biomedical research, it is important to consider two criteria: explainability/interpretability and generalizability. Many conventional state-of-the-art algorithms, such as neural networks, are seen as "black boxes" due to the low interpretability of the values and interactions of intermediate neurons deep within the network. Such algorithms thus have low explainability and are not ideal for research, where the ultimate goal is not performance but rather acquiring a more sophisticated understanding of relationships between variables. Furthermore, a major challenge posed by multi-omics data, in particular, is the lack of generalizability of learned models due to the heterogeneity, high-dimensionality,

[1]KBR, Moffett Field, CA, USA. [2]NASA Space Life Sciences Training Program, Moffett Field, CA, USA. [3]College of Letters and Science, University of California at Davis, Davis, CA, USA. [4]Space Biosciences Division, NASA Ames Research Center, Moffett Field, CA, USA. [5]Monash Proteomics and Metabolomics Platform, Monash Biomedicine Discovery Institute, Monash University, Clayton, VIC 3800, Australia. [6]Blue Marble Space, Seattle, WA, USA. [7]Abzu ApS, Copenhagen, Denmark. [8]Department of Marine Sciences, University of Georgia, Athens, GA, USA. [9]Department of Kinesiology, Centre for Bone and Muscle Health, Brock University, St. Catharines, Canada. [10]These authors contributed equally: Kevin Li, Riya Desai. ✉email: lauren.m.sanders@nasa.gov; sylvain.v.costes@nasa.gov

a

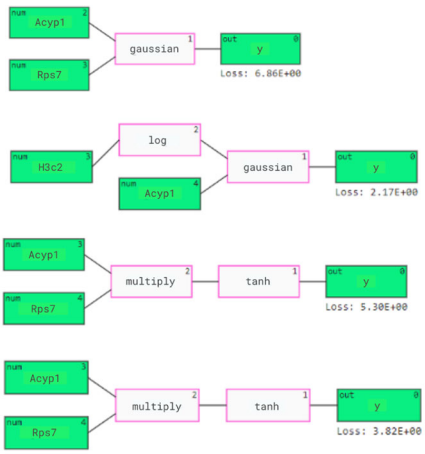

b

Feature	Models (n)
Acyp1 (proteomics)	89
Rps7 (proteomics)	27
Cct6a (proteomics)	5
Glt28d2 (RNA-seq)	4
Eml1 (proteomics)	3
Ehd2 (proteomics)	3
Tubb2c (proteomics)	3
Abat (RNA-seq)	3
Etv6 (RNA-seq)	3

c

T1 CV R^2	0.894
T10 CV R^2	0.711
RNA-seq features (n)	12
Proteomic features (n)	38

d

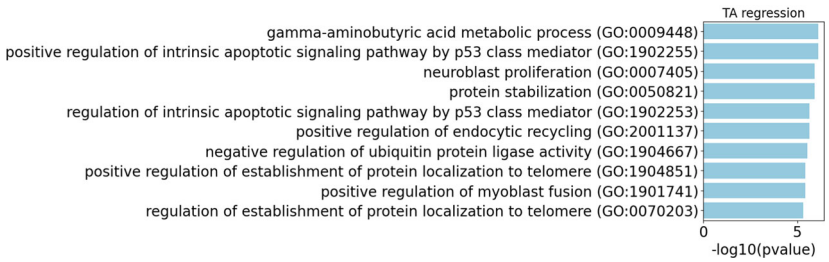

Fig. 1 QLattice regression analysis of TA multi-omics data and calcium uptake. a Representative examples of the mathematical relationships between multi-omic features identified by QLattice to predict calcium reuptake in TA muscle during LOOCV. **b** Top 9 features ranked by how many times they were used in a model found by QLattice during LOOCV. **c** T1 and T10 cross-validated R^2 scores, as well as the number of RNA-seq and proteomic features that were found among the top 50 features. **d** Gene set enrichment analysis results using the top nine genes from the QLattice analysis.

and low-sample-size (HDLSS) nature of the data. Highly expressive algorithms like neural networks will generate severely overfit models when trained on HDLSS data[6].

With these criteria in mind, we chose to use a recently developed implementation of symbolic regression called QLattice, developed by Abzu ApS[7,8]. Symbolic regression attempts to find the true, concise mathematical function directly underlying the features' relationship to the target, which is much more interpretable than neural network architectures and less likely to overfit. It does this by representing mathematical expressions as computational graphs, where the nodes represent variables or functions, and by exploring the possible architectures for these computational graphs. QLattice explores this graph space efficiently to find concise, interpretable, and accurate models, which make it a suitable tool for biomarker discovery[9].

We aimed to identify molecular drivers of spaceflight effects on muscle physiology using spaceflight mouse muscle data from the NASA Open Science Data Repository (OSDR) with omics data found in GeneLab[10,11] and Ca^{2+} reuptake data found in Ames Life Sciences Data Archive (ALSDA)[12]. First, we trained QLattice to predict calcium reuptake levels of spaceflight and ground control mice using multi-omics features (genes, proteins, etc.), a regression task. Second, we trained QLattice to predict whether samples were from spaceflight or ground control mice, a classification task. We then identified features that contributed most to the predictive capabilities of the model's output by QLattice; these features (i.e., genes, proteins, or epigenetic markers) are potential biomarkers that may provide mechanistic insight behind the spaceflight-induced muscle physiology effects and serve as targets for future interventions aiming to reduce the extent of muscle atrophy during space travel.

RESULTS

Multi-omics biomarkers associated with spaceflight calcium reuptake aberrations are revealed by machine learning regression analysis

Exposure to spaceflight has been previously reported to increase Ca^{2+} uptake in mouse TA muscles and decrease Ca^{2+} uptake in mouse SOL muscles[1]. We hypothesized that this phenotypic change can be further understood by examining the relationships between genes, proteins, and methylation markers. Therefore, we trained QLattice to identify multi-omics biomarkers predictive of changes in calcium reuptake capacity, using multi-omics datasets from OSD-104 mouse SOL muscle and OSD-105 mouse TA muscle from female C57BL/6J mice flown at 16 weeks of age on the RR-1 mission. For each muscle type, multi-omics data were combined and subject to dimensionality reduction prior to QLattice training, and calcium reuptake levels were used as a target (see Methods and Supplementary Information). We matched RR-1 SOL multi-omics data with RR-1 SOL calcium data and RR-1 TA multi-omics data with RR-9 TA calcium data. In the latter case, note that RR-9 includes 10-week male mice while RR-1 includes 16-week female mice, but we hypothesized that the spaceflight muscle effect would be great enough to overcome these differences. More details are provided in the Methods and Supplementary Information.

In the TA regression analysis reported here (Fig. 1), we used both RNA sequencing (RNA-seq) and proteomics data. We excluded the methylation data because including it reduced QLattice performance while producing very similar results (see Supplementary Information). The top two features predictive of Ca^{2+} uptake rate were Acyp1 and Rps7 proteins (Fig. 1b). Representative models containing Acyp1 and Rps7 are shown in Fig. 1a. These models consisted of bivariate Gaussian functions, bivariate multiply functions, and univariate tanh functions (see

a

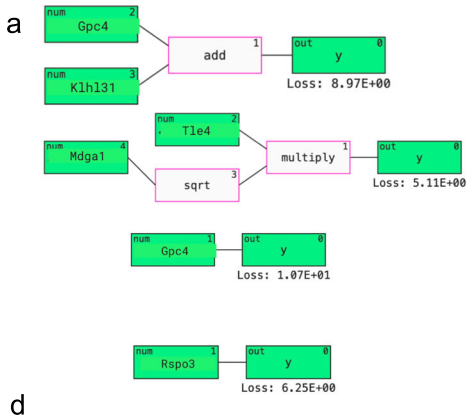

b

Feature	Models (n)
Gm35576 (RNA-seq)	12
Rspo3 (RNA-seq)	10
Gpc4 (RNA-seq)	5
Klhl31 (RNA-seq)	5
Sox6 (RNA-seq)	4
Auts2 (RNA-seq)	4
Sobp (RNA-seq)	3
Mdga1 (RNA-seq)	3
Aox1 (RNA-seq)	3
Tle4 (RNA-seq)	3
Klhl33 (RNA-seq)	3
Eepd1 (RNA-seq)	3
Rhbdl3 (RNA-seq)	3

c

T1 CV R^2	0.774
T10 CV R^2	0.766
RNA-seq features (n)	47
Methylation features (n)	3

d

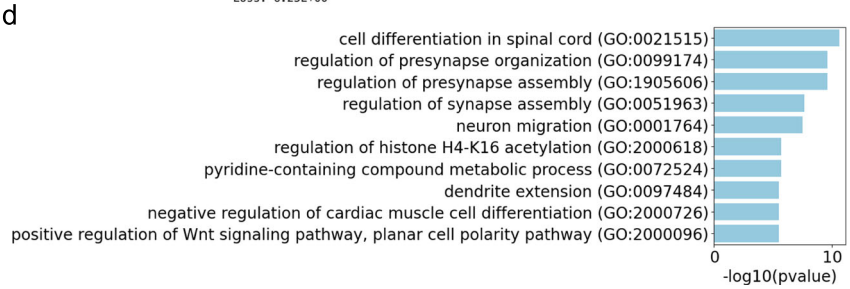

Fig. 2 QLattice regression analysis of SOL multi-omics data and calcium uptake. a Representative examples of the mathematical relationships between multi-omic features identified by QLattice to predict calcium reuptake in SOL muscle during LOOCV. **b** Top 13 features ranked by how many times they were used in a model found by QLattice during LOOCV. **c** T1 and T10 cross-validated R^2 scores, as well as the number of RNA-seq and methylation features that were found among the top 50 features. **d** Gene set enrichment analysis results using the top 13 genes from the QLattice analysis.

Supplementary Information for additional discussion of model architectures). Of the 27 models containing Rps7, 24 included a relationship with Acyp1, possibly indicating a biological interaction between the two features that could be tested in the future through laboratory studies. Gene set enrichment analysis revealed significant enrichment of biological signaling involved in apoptosis, endocytosis, and protein localization (Fig. 1d).

In the SOL regression analysis, the best-performing models mainly displayed relationships between the expression of different genes on the RNA level, related by mathematical functions such as Gaussian, linear, and exp (Fig. 2a–c). We focused on the top 13 features across all models by rank, all of which were RNA-seq features: *Gm35576, Rspo3, Gpc4, Klhl31, Sox6, Auts2, Sobp, Mdga1, Aox1, Tle4, Klhl33, Eepd1, Rhbdl3*, and *Gm21955*. Gene set enrichment analysis revealed significant enrichment of biological signaling involved in cellular differentiation, synapse organization and assembly, and neuron migration (Fig. 2d).

QLattice analysis identified 9 and 13 critical genes playing an important role in calcium reuptake of TA and SOL muscles, respectively, in the context of spaceflight-inducing muscle loss. Figure 3 depicts the changes of expression level in FLT versus GC for some of these genes and their corresponding proteins (when measurements are available) in both muscle types. Many of the genes identified have been described in the literature as playing a role in muscle recovery and we focus our attention on these genes.

In the case of TA muscle, Acyp1 protein was found in 89 models. Acyp1 has been shown to inhibit the activity of Ca2+ transporters in non-phospholamban-associated calcium-dependent ATPases, such as SERCA-1, which is predominantly found in fast-twitch muscle fibers, the dominant fiber type in the TA muscle[13–15]. In line with this, Acyp1 protein expression is negatively correlated with calcium reuptake in QLattice models for TA muscles (Supplementary Fig. 9), indicating that high levels of Acyp1 are associated with low calcium reuptake efficiency AUC. Consistent with previous studies[1], FLT TA samples exhibit lower Acyp1 protein expression and improved calcium reuptake (Fig. 3a, e). Interestingly, *Acyp1* gene expression in TA has a much greater spread across samples resulting in no significant difference between FLT and GC (Fig. 3b), possibly indicating a more reliable measurement from proteomics than RNA-seq.

Furthermore, Acyp1 has been shown to enhance the activity of Ca2+ transporters in phospholamban-associated calcium-ATPases, including SERCA-2a, which is predominantly found in slow-twitch fibers, the dominant fiber type in SOL muscle. We examined whether this pattern is consistent in the OSD-104 SOL multi-omics data and discovered that *Acyp1* gene expression was also downregulated in SOL FLT relative to GC (Fig. 3c), while calcium reuptake was impaired in SOL as previously reported[1] (Fig. 3g). Note that QLattice was not trained to find this association for SOL muscle. Such a finding is, therefore, quite strong, suggesting a potential mechanism. The observed downregulation in *Acyp1* could contribute to impairments in SERCA function found in the FLT SOL, as it is known that phospholamban is highly expressed in this muscle and is less expressed in fast glycolytic muscles. Taken together, these findings suggest that Acyp1 may play a mechanistic role in the dysregulation of calcium induced by spaceflight (Fig. 3d, f), but additional research is necessary to establish this relationship.

The second key protein identified in TA muscle was Rps7. This gene is known to be downregulated by nitrosative stress[16], which is related to impaired calcium reuptake[1]. Consistent with this, Rps7 is positively correlated with calcium reuptake capacity efficiency in the QLattice models (negatively associated with calcium reuptake AUC; Supplementary Fig. 9). This suggests a potential role for Rps7 in the calcium reuptake response to nitrosative stress. No nitrosative stress was reported in the TA samples from the original study[1], suggesting that mechanisms possibly including Rps7 may have enhanced the calcium reuptake efficiency. Further studies would be required to establish these relationships.

The QLattice analysis for SOL revealed a very distinct set of genes (Fig. 2b). This is, however, not surprising as only gene

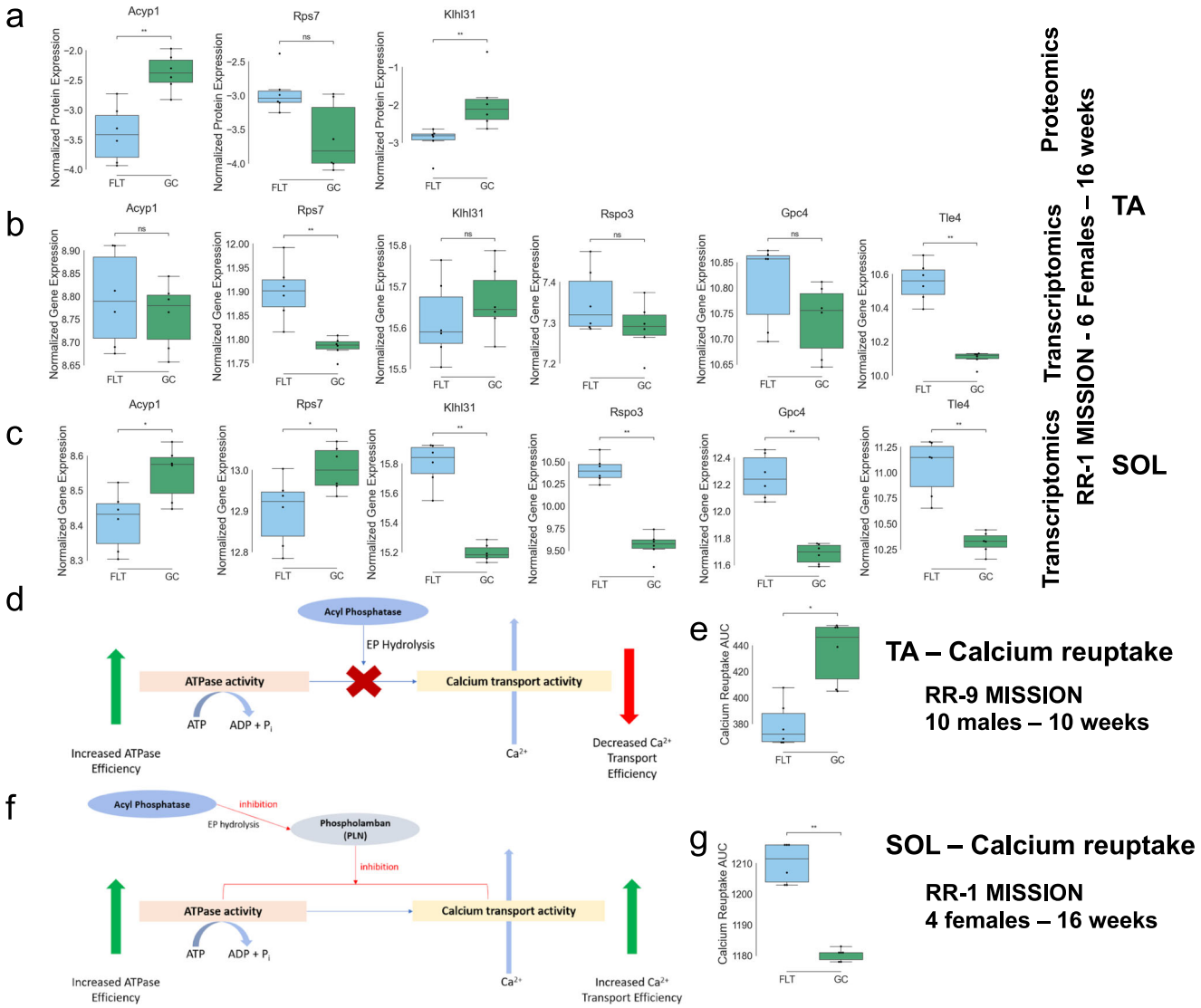

Fig. 3 Gene/protein relationship with calcium reuptake in SOL and TA muscles and putative mechanism. The expression levels of the top key genes identified by QLattice analysis and their corresponding protein levels are shown against the calcium reuptake AUC in both TA and SOL muscles flown in space (FLT) or from ground controls (GC). **a** QLattice key protein levels in TA. **b** QLattice key gene expression levels in TA. **c** QLattice key gene expression levels in SOL. **d** Putative mechanism based on the Acyp1 response, showing up in the majority of the models for TA muscle and **e** SOL muscle. **f** Calcium reuptake AUC in TA muscle. **g** Calcium reuptake AUC in SOL muscle. All significance was calculated using Mann–Whitney–Wilcoxon test two-sided: *: 1.00e−02 < $p \leq$ 5.00e−02, **:1.00e−03 < $p \leq$ 1.00e−02).

expression and methylation data were available. Several of these genes are already known for their relationship to calcium reuptake efficiency and muscle response to injury, and their levels are plotted for protein expression (when available) and gene expression in both TA and SOL muscle in Fig. 3a–c. *Gpc4* is underexpressed in injury-activated muscle satellite cells[17]; similarly, *Tle4* is normally underexpressed following muscle injury to allow myogenesis[18]. In our data, both *Tle4* and *Gpc4* were upregulated in mouse FLT SOL (Fig. 3a, b), which displayed impaired calcium reuptake vs. GC SOL (Fig. 3g). This may indicate that failure of proper *Gpc4* and *Tle4* downregulation may play a role in damaged calcium reuptake, possibly by lowering overall muscle quality. This is supported by previous RNA-seq data showing that genes involved with myogenesis and differentiation were downregulated in the FLT SOL from mice[19]. Alternatively, *Tle4* expression is known to be triggered by calcium signaling[20], so the observed *Tle4* upregulation may instead be the result of increased cytoplasmic calcium levels due to impaired reuptake.

Further, *Rspo3* has been found to be one of the most upregulated genes after SOL training and is associated with a decrease in muscle atrophy[21], and its knockout has shown to compromise myogenesis and myotube differentiation[22]. Similarly, mice lacking *Klhl31* exhibit stunted skeletal muscle growth, centronuclear myopathy, and SR dilation[23]. In our data, both *Rspo3* and *Klhl31* are also upregulated in SOL FLT samples with lower calcium reuptake ability (Fig. 3c), possibly as a compensatory or adaptive mechanism to increased calcium levels due to decreased uptake[24].

Multi-omics biomarkers associated with spaceflight calcium reuptake aberrations are revealed by ML classification analysis

We then hypothesized that there may be other molecular pathways affected by spaceflight in mouse muscle that could be identified through feature relationships in QLattice models. Therefore, we broadened the scope of our analysis to identify

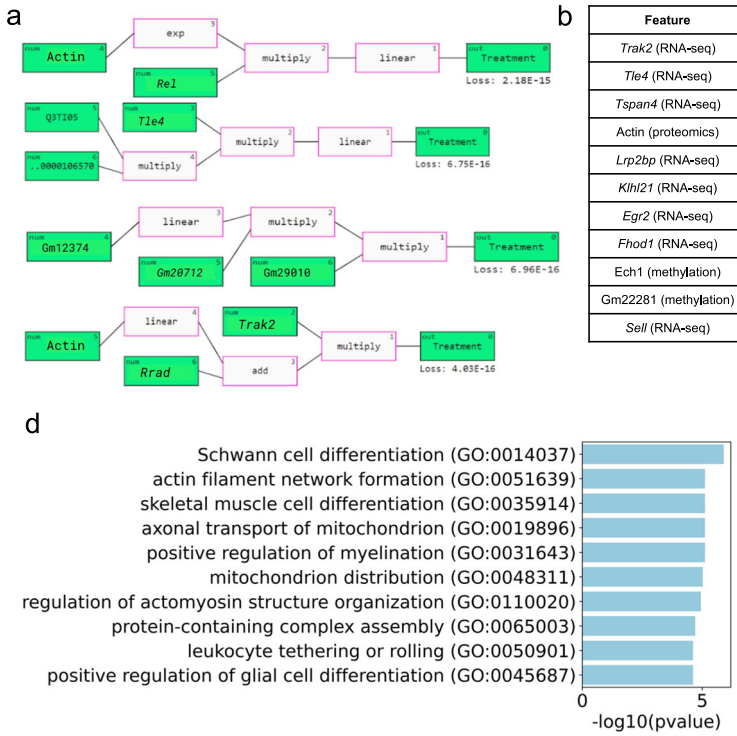

Feature	Models (n)
Trak2 (RNA-seq)	20
Tle4 (RNA-seq)	14
Tspan4 (RNA-seq)	12
Actin (proteomics)	11
Lrp2bp (RNA-seq)	8
Klhl21 (RNA-seq)	8
Egr2 (RNA-seq)	7
Fhod1 (RNA-seq)	6
Ech1 (methylation)	5
Gm22281 (methylation)	5
Sell (RNA-seq)	5

T1 CV R^2	1.0
T10 CV R^2	0.997
RNA-seq features (n)	25
Proteomics features (n)	16
Methylation features (n)	59

Fig. 4 QLattice classification analysis of TA multi-omics data and FLT/GC groups. a Representative examples of the mathematical relationships between multi-omic features identified by QLattice to predict FLT versus GC in TA muscle during LOOCV. **b** Top 11 features ranked by how many times they were used in a model found by QLattice during LOOCV. **c** T1 and T10 cross-validated R^2 scores, as well as the total number of RNA-seq, proteomics, and methylation features across all models. **d** Gene set enrichment analysis results using the top 11 features from the QLattice analysis.

multi-omics features that were predictive of the FLT or GC groups rather than restricting to a single phenotype. We used QLattice to classify FLT samples from GC and assessed the resulting models and feature interactions.

In the TA classification analysis, we used all 3 types of omics data: RNA-seq, proteomics, and methylation data (Fig. 4a–c). The top 11 features from this analysis included all 3 types of features: *Trak2* (RNA-seq), *Tle4* (RNA-seq), *Tspan4* (RNA-seq), Actin (Proteomic), Gm22281 (Methylation), *Sell* (RNA-seq), Ech1 (Methylation), *Fhod1* (RNA-seq), *Egr2* (RNA-seq), *Klhl21* (RNA-seq), and *Lrp2bp* (RNA-seq).

In keeping with our hypothesis, gene set enrichment analysis revealed significant enrichment of pathways relevant to muscle biology and the neuromuscular response to stress, including skeletal muscle cell differentiation, positive regulation of myelination, and Schwann cell differentiation (Fig. 4d). Interestingly, multiple pathways involved mitochondrial regulation, which has been previously identified as a molecular response to spaceflight in multiple tissues including muscle[25].

The pathway analysis also uncovered perturbation of actin and myosin structural regulation. The actin protein was the top proteomics feature found across QLattice models (Fig. 4b) and was upregulated in TA FLT samples (Fig. 5a). Actin is a key component in the myofibril bundles which generate muscle contractions after Ca^{2+} release and signaling[26]. Further, the top RNA-seq feature *Trak2* is known to enable myosin binding activity for muscle contraction[27]. *Trak2* is also involved in the Rho GTPase cycle, which plays an important role in muscle mass regeneration and myofibrillogenesis[27]. The *Trak2* gene is upregulated in FLT TA muscle in our data (Fig. 5b), possibly as a muscle regeneration mechanism in a weightless environment. *Tle4*, the second highest occurring RNA-seq feature across all QLattice models, acts as a corepressor regulating muscle cell differentiation[18]. The *Tle4* gene is upregulated in FLT TA muscle in our data (Fig. 5b), possibly due to the lack of a need for skeletal muscle growth in a weightless environment.

Interestingly, both *Trak2* and *Tle4* displayed some co-occurrence with Actin. Out of the 20 models that *Trak2* appeared in, 4 of them contained Actin, while out of the 14 models containing *Tle4*, 2 of them contained Actin. This may indicate a co-regulation network between Actin structural muscle activity and muscle mass regeneration and cell differentiation in response to spaceflight, which could be further investigated in laboratory studies.

In the SOL classification analysis, RNA-seq gene features comprised 69 out of the 80 features across all resulting models (Fig. 6a–c). The top 9 recurrent features were *Fam220a*, *Lrp4*, *Osgin2*, *Gm29686, Gm22281* (Methylation), *Sema6c*, *Alpk3*, *Tmod1*, and *Bcam*. For the most part, these features appeared in single-feature models related to the FLT/GC outcome by a linear, log, or inverse relationship. Of the 120 total models, 18 described relationships between 2 features. Interestingly, 11 of these were pairs of methylation and RNA-seq features, indicating a potential cooperative relationship between gene expression and DNA methylation in spaceflight SOL muscle response.

Similar to the calcium reuptake prediction analysis, the SOL FLT/GC classification analysis mainly identified models with interactions between RNA-seq gene features. Gene set enrichment analysis of the top 11 features revealed enrichment of pre- and post-synaptic membrane assembly and organization (Fig. 6d), in keeping with previous research showing structural alterations in muscle synaptic organization in spaceflight[28].

DISCUSSION

Here we report the identification of multi-omics biomarkers in mouse SOL or TA muscle that are predictive of change in calcium reuptake capacity during spaceflight or broadly predictive of molecular changes in spaceflight samples compared to ground

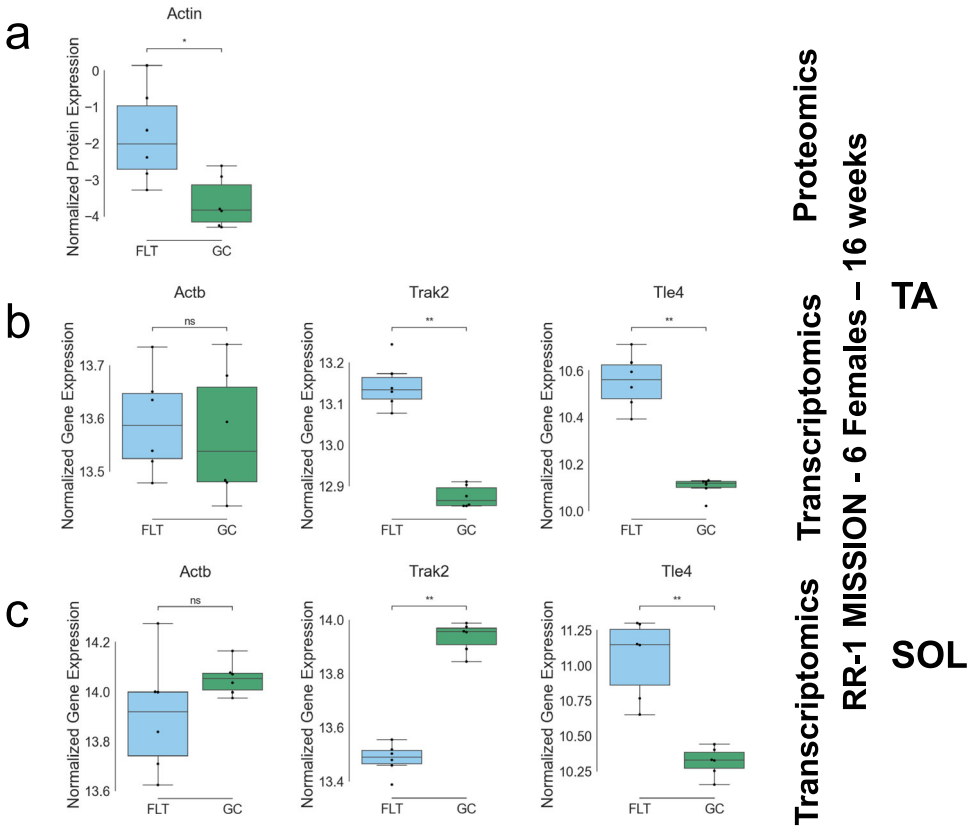

Fig. 5 Expression levels of top proteins and genes identified by QLattice TA and SOL classification analysis and muscle weights. **a** QLattice key protein levels in TA. **b** QLattice key gene levels in TA. **c** QLattice key gene levels in SOL. All significance was calculated using Mann–Whitney–Wilcoxon test two-sided: *: 1.00e−02 < $p \leq$ 5.00e−02, **:1.00e−03 < $p \leq$ 1.00e−02).

control. Our study is a key contribution to the field both in the identification of these biomarkers and in that we demonstrate the utility of ML methodology for biomarker discovery in space biology by using the QLattice symbolic regression method to characterize biomarker relationships to each other and to the predictive target. Instead of using the traditional systems biology approach, ML methods provide unbiased identification of potential candidates for biological mechanisms. Our study is also one of the first to analyze combined multi-omics and non-omics/phenotypic data from the NASA OSDR, leveraging the relational database structure, which allows for mapping samples across assays and missions.

Appropriate regulation of muscular cytoplasmic calcium levels is key for several downstream calcium-dependent signaling pathways. Calcium reuptake is reportedly improved in TA muscle but impaired in SOL muscle, during spaceflight[1], with limited understanding of the molecular signaling causing these phenotypic changes. Here, we report that enhanced Ca^{2+} uptake in FLT TA is directly related to the combined interaction of Acyp1 protein downregulation and Rps7 protein upregulation; while decreased Ca^{2+} uptake in FLT SOL is related to interactions of upregulation of several different pairs of genes, including *Gpc4*, *Tle4*, *Rspo3*, and *Klhl31*. The lower Ca^{2+} uptake in FLT SOL is also correlated with significant weight loss for the SOL muscle in the RR1 flight samples (*t*-test *p*-value < 0.05); whereas there is no significant change in weight for TA muscles (Table 1). Overall, the analysis provided here suggests that TA muscles are more resilient to space conditions, and Acyp1 and Rps7 seem to be good candidates to counteract weight losses and poor Ca^{2+} uptake observed in SOL muscles.

On the technological aspect of this work, we show that one of the major advantages of QLattice compared to traditional multi-omics or differential gene expression analysis methods is its ability to elucidate a variety of mathematical interactions, not necessarily linear, between different multi-omics features. We noted a variety of mathematical functions in the QLattice models from our analysis, including bivariate Gaussian, bivariate multiply, univariate tanh, addition, multiplication, and log. The response plots provided by QLattice help translate the mathematical functions into biological and mechanistic interpretations (Supplementary Fig. 9). We noted that when Gaussian functions are reported, only the first half of the Gaussian curve is being used to fit a sigmoidal trend (Supplementary Fig. 9). Biologically, we interpret this to be because biological quantities (e.g., calcium concentration) cannot be negative, nor cannot exceed a certain threshold (e.g., the total amount of calcium stored in the sarcoplasmic reticulum). Thus, linear models would actually fail to extrapolate in these more extreme ends of the quantity's range, while sigmoidal models would fit much more accurately. To further improve the predictive capability of this tool, it would be valuable to further characterize the relationship between the mathematical functions identified by QLattice and the distribution of protein concentrations in various tissues. Such characteristics would help further translate the interactions of the various functions found in QLattice with an actual biological process between different key components of a tissue.

While additional study is needed to fully characterize the relationships identified here by QLattice, we suggest that QLattice's emphasis on concise, interpretable models makes it an especially appropriate ML methodology for research applications where explainability is key. Biomedical research, and especially space biology research, presents the additional challenge of small sample sizes, which usually leads to severe overfitting and a lack of generalizability in the models found by

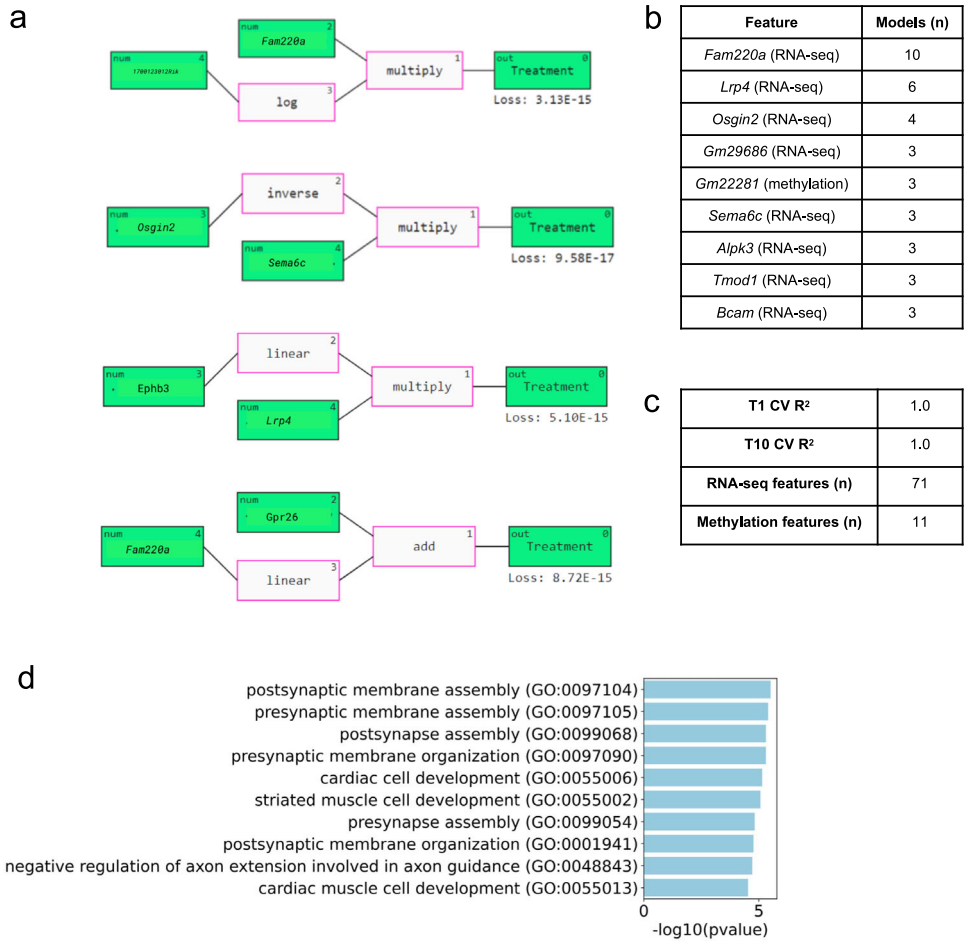

Feature	Models (n)
Fam220a (RNA-seq)	10
Lrp4 (RNA-seq)	6
Osgin2 (RNA-seq)	4
Gm29686 (RNA-seq)	3
Gm22281 (methylation)	3
Sema6c (RNA-seq)	3
Alpk3 (RNA-seq)	3
Tmod1 (RNA-seq)	3
Bcam (RNA-seq)	3

T1 CV R^2	1.0
T10 CV R^2	1.0
RNA-seq features (n)	71
Methylation features (n)	11

Fig. 6 QLattice classification analysis of SOL multi-omics data and FLT/GC groups. a Representative examples of the mathematical relationships between multi-omic features identified by QLattice to predict FLT versus GC in SOL muscle during LOOCV. **b** Top 9 features ranked by how many times they were used in a model found by QLattice during LOOCV. **c** T1 and T10 cross-validated R^2 scores, as well as the total number of RNA-seq and methylation features across all models. **d** Gene set enrichment analysis results using the top 9 features from the QLattice analysis.

Table 1. Average processed tissue weights for RR-1 SOL and TA groups.

	Condition	Average weight (mg)
RR-1 SOL	FLT	7.9
	GC	10.5
RR-1 TA	FLT	13.3
	GC	13.9

conventional ML algorithms. This issue is at least partially addressed by QLattice's predisposition to limit the architectural complexity of models (which has a strong regularizing effect), as well as its heavy intrinsic feature selection based on mutual information with the target variable. A valuable future study would be to characterize the relationship between the individual data modalities and the overall multi-omics results.

As demonstrated in this study, when an ML method properly accounts for these challenges and priorities specific to space biology research, it can provide significant guidance for what to focus on in future research. Although the top biomarkers from QLattice must be further characterized and confirmed, the method has appreciably narrowed the research "search space" by directing us toward groups of biomarkers that are most promising. In this way, explainable and interpretable ML, with its advantage over humans in being able to process huge feature spaces, serves as a metaphorical "metal detector," telling us where we should start digging. The results we report here would benefit from future experimental validation studies.

We conclude with our observations on the contributions of the different types of omics data to the QLattice predictive models. In this work, DNA methylation CpG+ features, when mapped to gene names or when maintained as genomic coordinates, failed to greatly contribute to model architectures and resulted in lower predictive performance. We suggest that this may be because methylation marks are deposited over time, so molecular changes during spaceflight are primarily dominated by functional changes, while small but persistent epigenetic changes may be better captured upon return to earth. To test this hypothesis, future studies could capture methylation measurements both before and after spaceflight from the same animals. In accordance with this hypothesis, both protein and gene expression changes were the most predictive features, with the top proteomic features much stronger and more cohesive than those of top RNA-seq features. This may constitute support in favor of focusing on proteomic analysis over RNA-seq analysis in future spaceflight studies, as the relationship between proteins and function is more immediate compared to the presumably noisier relationship between transcripts and function.

Taken together, our results build on previous work in the field by reporting a promising demonstration of an explainable ML method for space biology research and providing several potential biomarkers for future study on muscle response to spaceflight.

METHODS

RNA sequencing data (RR-1—SOL and TA muscles—female)

For RNA-seq RR-1 data, we started with the raw count files available on OSDR from the GeneLab RNA-seq processing pipeline[29]. We filtered out lowly expressed genes with unreliable reads (i.e., we only kept genes that had at least 10 non-zero reads in at least 3 samples), resulting in a reduction of dimensionality from 55,536 genes to 15,848 genes for OSD-104 and 16,660 genes for OSD-105, with an overlap of 15,216 genes between the two datasets (Supplementary Fig. 5g). We then applied a variance-stabilizing transformation (VST) using DESeq2 v1.34.0[30], which corrected for library size/sequencing depth and mitigated heteroskedasticity and skewed distributions. The mean-variance relationship and count distribution were checked post-normalization to confirm the effectiveness of preprocessing (Supplementary Fig. 1a–d, Supplementary Fig. 3a–d). Within- and across-group gene expression variance distributions show greater variance spread for the FLT samples than the GC samples (Supplementary Fig. 5a–f).

Proteomics data (RR-1—TA muscle only—female)

The proteomics data for OSD-105 was collected in two runs of TMT-labeled mass spectrometry with a bridge channel in each run consisting of a pooled sample of all FLT and GC samples[31]. To ensure values were comparable when combining the runs, we used the ratio of expression values for each sample relative to that of the corresponding bridge channel. After combining the data from the runs, we performed a log2 transformation of the expression values, filtered out proteins with too many missing values, and applied VST normalization, all using the DEP v1.16.0R package[32]. Again, the mean-variance relationship and distribution were checked (Supplementary Fig. 1e, f, Supplementary Fig. 3e, f). We then imputed missing data using K-nearest neighbor imputation, which did not significantly affect the distribution (Supplementary Fig. 4a, c). Finally, we removed any remaining batch effects between the two runs that were amplified through the preprocessing steps using methods from the limma v3.50.3R package, which are appropriate to apply on properly transformed proteomics data[33]. The removal of batch effects was confirmed using paired PCA plots of the top principal components (PCs) (Supplementary Fig. 4b, d). The preprocessed dataset contained 1786 proteins.

Bisulfite sequencing data (RR-1—SOL and TA muscle—female)

Raw bisulfite sequencing FASTQ files were processed using the Nextflow nf-core methylseq pipeline (v1.6.1), which uses the Bismark aligner for genome alignment and extracting methylation calls (Supplementary Fig. 2a)[34,35]. The processed data were filtered to only CpG-type methylated sites, as non-CpG methylation is usually restricted to a few specific cell types (e.g., pluripotent stem cells, glial cells, neurons) that are not as relevant in this context (Supplementary Fig. 2b–d)[36]. The methylation sites were then mapped to their corresponding genes. For each methylation site, we found the gene whose chromosomal range included the site. Methylation sites that didn't fall into annotated gene regions were discarded, as the current study focuses on mechanistic relationships between coding features. We then calculated the percentage of CpG sites in each gene that was methylated (% methylation). There were 48,368 and 47,660 methylation features for OSD-104 and OSD-105, respectively, after preprocessing (distributions shown in Supplementary Fig. 4e, f). We experimented with using site-level methylation features instead of gene-level methylation features, but this resulted in severe overfitting of ML models. The remaining methylation features overlap with the majority of the genes measured in the RNA-seq datasets, although a majority of the methylation loci do not map to an RNA-seq gene (Supplementary Fig. 5g). In order to assess whether the loci with the highest percent methylation are related to the genes with the lowest expression, as would be expected mechanistically, we compared the top 10% methylated genes with the bottom 10% expressed genes (Supplementary Fig. 5h). There is some limited overlap but less than would be expected considering the overlap of all genes and methylated loci.

Calcium reuptake data (RR-1 SOL female, RR-9 TA male)

Calcium reuptake data was acquired from OSDR dataset OSD-488[37], which contains rates of $Ca2+$ uptake in the muscle homogenates measured in a 96-well plate using the Indo-1 $Ca2+$ fluorophore[1]. These values were collected as a time series, with the measurements of cytoplasmic calcium concentrations taken at multiple points in time during a period of muscle relaxation. For our analysis, we use the area under the curve (AUC) as a measurement of calcium reuptake change over time. A lower AUC value implies more efficient calcium reuptake.

For this study, we did not have multi-omics and calcium uptake measurements from the same animals. Therefore, for comparing omics and calcium uptake data, we assigned calcium reuptake values to omics samples based on perturbation analysis to identify the optimal pairing (see Supplementary Information, Supplementary Fig. 8). It is well characterized that there are significant physiological and molecular differences between muscle samples from spaceflight and ground samples[1,2]. We inferred that this difference would be greater than within-group differences in mission, age, and sex and would allow us to identify the spaceflight effect relationship between omics features and calcium uptake. Specifically, the SOL calcium reuptake measurements were collected from age- and sex-matched mice from the same RR-1 cohort as the OSD-104 SOL omics data. There was no TA calcium reuptake measurement done in the RR-1 cohort; the OSD-488 dataset only had TA calcium reuptake measurements collected from 10-week-old male mice flown on the RR-9 mission. We, therefore, paired the TA muscles calcium reuptake from these 10-week-old male mice with the OSD-105 TA multi-omics data, which are from older females.

Model hyperparameters

The primary hyperparameters for QLattice (*feyn* package v3.0.2) were the number of epochs and the maximum complexity of the architectures. The number of epochs corresponded to the number of generations for the evolutionary search algorithm as a whole rather than the number of epochs of backpropagation for any individual model architecture being explored. We tried various values for the number of epochs between 10 and 100, but there were no significant differences in validation performance or feature rankings. The maximum architectural complexity was restricted to 4 (2 features and 2 functional interactions) for the SOL analysis since SOL data had two data types, and we were interested in modeling the interactions between the data types. Similarly, the maximum architectural complexity was restricted to 6 for the TA analysis.

Statistical analysis

Gene set enrichment analysis was performed using the Enrichr implementation in the *gseapy* library (v0.10.4) in Python, using GO_Biological_Process_2021 as the background gene set. Boxplots were generated using *seaborn* (v0.11.2) in Python, with statistical annotations calculated using the *statannotations*

package (v0.5.0) implementation of the Mann–Whitney–Wilcoxon two-sided test.

Reporting summary

Further information on research design is available in the Nature Research Reporting Summary linked to this article.

DATA AVAILABILITY

The datasets used in this study were collected from the NASA Rodent Research 1 (RR-1) and 9 (RR-9) missions and are publicly available on the NASA OSDR (osdr.nasa.gov). RR-1 samples were from female C57BL/6 J mice flown at 16 weeks of age for 37 days. RR-9 samples were from male C57BL/6 J mice flown at 10 weeks of age for 35 days. Specifically, we used datasets OSD-104 (RR-1 multi-omics mouse SOL data)[31], OSD-105 (RR-1 multi-omics mouse TA data)[38], and OSD-488 (RR-1 and RR-9 calcium reuptake data)[37]. OSD-104 dataset consists of bulk RNA-seq and bisulfite sequencing DNA methylation data for SOL muscle samples collected from 6 space-flown mice (FLT) and 6 ground control mice (GC) during the RR-1 mission[38]. OSD-105 dataset consists of bulk RNA-seq, bisulfite sequencing DNA methylation, and mass-spectrometry-based proteomics data for TA muscle samples, also collected from 6 FLT and 6 GC mice during RR-1[31]. OSD-488 dataset[1,37] originates from a study consisting of calcium reuptake data from female SOL muscle samples collected from 4 FLT and 4 GC during the RR-1 mission; 10 FLT and 10 GC of SOL and TA male muscle samples during the RR-9 mission.

CODE AVAILABILITY

Due to the NASA Software Release requirements, the code for this study is not publicly available.

Received: 15 April 2023; Accepted: 21 November 2023;
Published online: 13 December 2023

REFERENCES

1. Braun, J. L., Geromella, M. S., Hamstra, S. I., Messner, H. N. & Fajardo, V. A. Characterizing SERCA function in murine skeletal muscles after 35-37 days of spaceflight. *Int. J. Mol. Sci.* **22** (2021).
2. Juhl, O. J. 4th et al. Update on the effects of microgravity on the musculoskeletal system. *NPJ Microgravity* **7**, 28 (2021).
3. Ulanova, A. et al. Isoform composition and gene expression of thick and thin filament proteins in striated muscles of mice after 30-day space flight. *Biomed. Res. Int.* **2015**, 104735 (2015).
4. Reel, P. S., Reel, S., Pearson, E., Trucco, E. & Jefferson, E. Using machine learning approaches for multi-omics data analysis: a review. *Biotechnol. Adv.* **49**, 107739 (2021).
5. Bzdok, D., Altman, N. & Krzywinski, M. Statistics versus machine learning. *Nat. Methods* **15**, 233–234 (2018).
6. Hastie, T., Tibshirani, R. & Friedman, J. *The Elements of Statistical Learning: Data Mining, Inference, and Prediction, Second Edition (Springer Series in Statistics)*. (Springer, 2016).
7. Broløs, K. R. et al. An approach to symbolic regression using Feyn. Preprint at *arXiv* https://doi.org/10.48550/arXiv.2104.05417 (2021).
8. Wilstrup, C. & Kasak, J. Symbolic regression outperforms other models for small data sets. Preprint at *arXiv* https://doi.org/10.48550/arXiv.2103.15147 (2021).
9. Christensen, N. J. et al. Identifying interactions in omics data for clinical biomarker discovery using symbolic regression. *Bioinformatics* **38**, 3749–3758 (2022).
10. Ray, S. et al. GeneLab: Omics database for spaceflight experiments. *Bioinformatics* **35**, 1753–1759 (2019).
11. Berrios, D. C., Galazka, J., Grigorev, K., Gebre, S. & Costes, S. V. NASA GeneLab: interfaces for the exploration of space omics data. *Nucleic Acids Res.* **49**, D1515–D1522 (2021).
12. Scott, R. T. et al. Advancing the integration of biosciences data sharing to further enable space exploration. *Cell Rep.* **33**, 108441 (2020).
13. Nediani, C. et al. A novel interaction mechanism accounting for different acylphosphatase effects on cardiac and fast twitch skeletal muscle sarcoplasmic reticulum calcium pumps. *FEBS Lett.* **443**, 308–312 (1999).
14. Nassi, P., Nediani, C., Liguri, G., Taddei, N. & Ramponi, G. Effects of acylphosphatase on the activity of erythrocyte membrane Ca2+ pump. *J. Biol. Chem.* **266**, 10867–10871 (1991).
15. Nediani, C., Marchetti, E., Liguri, G. & Nassi, P. Alterations induced by acylphosphatase in the activity of heart sarcolemma calcium pump. *Biochem. Int.* **26**, 715–723 (1992).
16. Yan, F. et al. Nitrosative stress induces downregulation of ribosomal protein genes via MYCT1 in vascular smooth muscle cells. *Eur. Rev. Med. Pharmacol. Sci.* **25**, 5653–5663 (2021).
17. Pisconti, A., Bernet, J. D. & Olwin, B. B. Syndecans in skeletal muscle development, regeneration and homeostasis. *Muscles Ligaments Tendons J.* **2**, 1–9 (2012).
18. Agarwal, M., Bharadwaj, A. & Mathew, S. J. TLE4 regulates muscle stem cell quiescence and skeletal muscle differentiation. *J. Cell Sci.* **135** (2022).
19. Cadena, S. M. et al. Skeletal muscle in MuRF1 null mice is not spared in low-gravity conditions, indicating atrophy proceeds by unique mechanisms in space. *Sci. Rep.* **9**, 9397 (2019).
20. Bandyopadhyay, S., Valdor, R. & Macian, F. Tle4 regulates epigenetic silencing of gamma interferon expression during effector T helper cell tolerance. *Mol. Cell. Biol.* **34**, 233–245 (2014).
21. Adams, C. M., Suneja, M., Dudley-Javoroski, S. & Shields, R. K. Altered mRNA expression after long-term soleus electrical stimulation training in humans with paralysis. *Muscle Nerve* **43**, 65–75 (2011).
22. Han, X. H., Jin, Y.-R., Seto, M. & Yoon, J. K. A WNT/β-catenin signaling activator, R-spondin, plays positive regulatory roles during skeletal myogenesis*. *J. Biol. Chem.* **286**, 10649–10659 (2011).
23. Papizan, J. B. et al. Deficiency in Kelch protein Klhl31 causes congenital myopathy in mice. *J. Clin. Invest.* **127**, 3730–3740 (2017).
24. Fajardo, V. A. *The Role of Phospholamban and Sarcolipin in Skeletal Muscle Disease*. (University of Waterloo, 2015).
25. da Silveira, W. A. et al. Comprehensive multi-omics analysis reveals mitochondrial stress as a central biological hub for spaceflight impact. *Cell* **183**, 1185–1201.e20 (2020).
26. Cooper, G. M. *Actin, Myosin, and Cell Movement*. (Sinauer Associates, 2000).
27. Rodríguez-Fdez, S. & Bustelo, X. R. Rho GTPases in skeletal muscle development and homeostasis. *Cells* **10** (2021).
28. Deschenes, M. R., Wilson, M. H. & Kraemer, W. J. Neuromuscular adaptations to spaceflight are specific to postural muscles. *Muscle Nerve* **31**, 468–474 (2005).
29. Overbey, E. G. et al. NASA GeneLab RNA-seq consensus pipeline: standardized processing of short-read RNA-seqdata. *iScience* **24**, 102361 (2021).
30. Anders, S. & Huber, W. Differential expression analysis for sequence count data. *Genome Biol.* **11**, R106 (2010).
31. Galazka, J. & Globus, R. OSD-105: Rodent Research-1 (RR1) NASA Validation Flight: Mouse tibialis anterior muscle transcriptomic, proteomic, and epigenomic data. https://doi.org/10.26030/xgw6-6t64 (2017).
32. Smits, A. & Huber, W. *DEP: Differential Enrichment analysis of Proteomics data*. https://doi.org/10.18129/B9.bioc.DEP.
33. Ritchie, M. E. et al. limma powers differential expression analyses for RNA-sequencing and microarray studies. *Nucleic Acids Res.* **43**, e47 (2015).
34. Ewels, P. A. et al. The nf-core framework for community-curated bioinformatics pipelines. *Nat. Biotechnol.* **38**, 276–278 (2020).
35. Ewels, P., Hammaren, R., Peltzer, A. & Huther, P. *nf-core methylseq*. https://doi.org/10.5281/zenodo.2555454.
36. Jang, H. S., Shin, W. J., Lee, J. E. & Do, J. T. CpG and Non-CpG methylation in epigenetic gene regulation and brain function. *Genes* **8** (2017).
37. Fajardo, V., Braun, J. L., Geromella, M. S. & Hamstra S. I., M. H. N. OSD-488: Characterizing SERCA Function in Murine Skeletal Muscles after 35-37 Days of Spaceflight from RR-1 and RR-9. https://doi.org/10.26030/3nve-tk61 (2023).
38. Galazka, J. & Globus, R. OSD-104: rodent Research-1 (RR1) NASA Validation Flight: Mouse soleus muscle transcriptomic and epigenomic data. https://doi.org/10.26030/em9r-w619 (2017).

ACKNOWLEDGEMENTS

Resources supporting this work were provided by the NASA High-End Computing (HEC) Program through the NASA Center for Climate Simulation (NCCS) at Goddard Space Flight Center. We acknowledge support from the Space Life Sciences Training Program. The Open Science Data Repository is funded by the Space Biology Program (Science Mission Directorate, Biological and Physical Sciences Division) of the National Aeronautics and Space Administration. Funding for open access charge: NASA.

AUTHOR CONTRIBUTIONS

K.L. and R.D. performed the analysis and wrote the paper. K.L. and R.D. contributed equally to this work and should be considered co-first authors. R.T.S., J.R.S., M.M., S.D., A.H., J.L.B., and V.A.F. provided expert input and contributed to the paper. L.M.S. and S.V.C. provided oversight and project direction and contributed to the paper. All authors read and approved the final paper.

COMPETING INTERESTS

The authors declare no competing interests.

ADDITIONAL INFORMATION

Supplementary information The online version contains supplementary material available at https://doi.org/10.1038/s41526-023-00337-5.

Correspondence and requests for materials should be addressed to Lauren M. Sanders or Sylvain V. Costes.

Reprints and permission information is available at http://www.nature.com/reprints

Publisher's note Springer Nature remains neutral with regard to jurisdictional claims in published maps and institutional affiliations.